Deep Learning Based Vessels and Optical Disc Segmentation in Retinopathy Images

Thesis Submitted By:

Mohsin Raza
01-243171-021

Supervised By:

Dr. Shehzad Khalid

A thesis submitted to the Department of Computer Science, Bahria University, Islamabad as a partial fulfillment of the requirements for the award of the degree of Masters in Computer Science

Session (2017-2019)

Abstract

Medical image processing is helping the human for the diagnosis of different diseases using artificial intelligence-based algorithms. Eye diseases such as glaucoma is based on segmentation of optical disc and blood vessels in retinopathy images. Diabetic retinopathy is a radical eye disease and it causes of blindness at adverse level. Optical disc and blood vessels commence nurturing at early stage of diabetic retinopathy recognized as proliferative diabetic retinopathy. The correct segmentation of blood vessels and optical disc help the medical specialist and ophthalmologists in primary recognition of vision related diseases like glaucoma, hypoxemia, diabetic retinopathy etc. The segmentation of retinal images is much dependent on image quality and illuminations. The image acquisition stage can create non-uniform illumination of the fundus images which can make the retinal vessel pixel closer to the background. The conventional schemes are much dependent image processing techniques to enhance the image prior to the segmentation process which require much time and processing cost. Deep learning is famous to help the computer vision task with accuracy and reliability. Therefore, in this study, we propose a new deep learning-based method for the segmentation of optic disc and blood vessels using convolutional neural network. The intensive segmentation task is carried out by semantic segmentation which enable the network to perform the reliable segmentation without the overhead of pre-processing.

The experiments include both retinal vessel and optical disc segmentation using publicly available datasets. The vessel segmentation experiment is performed with famous DRIVE dataset, whereas the optical disc segmentation experiment is performed with MESSIDOR dataset. The experimental results show the fine segmentation performance of proposed method for both vessel and optical disc segmentation in order to support the diagnosis in retinal diseases.

Acknowledgments

Firstly i would thank Allah swt who helped me throughout this journey. I would like to show my warm thank to my supervisor Dr Shezad Khalid, who supported me at every bit and without whom it was impossible to accomplish the end task

I would like to extend thanks all the faculty and staff members of Computer Science Department, whose services turned my research a success.

Lastly, I would like to acknowledge my Mom and Dad, family members and friends, without whom I was nothing; they not only assisted me financially but also extended their support morally and emotionally.

Mohsin Raza

Bahria University Islamabad, Pakistan

July 2019

Contents

List of Figures

List of Tables

Acronyms and Abbreviations

CNN	Convolutional neural network
FCNN	Fully convolutional neural network
ANN	Artificial neural network
SVM	Support Vector Machine
PDR	Proliferative diabetic retinopathy
NPDR	Non-proliferative diabetic retinopathy
DR	Diabetic retinopathy
MRI	Magnetic resonance imaging
FOV	Field of view
RBF	Radial basis function
A/V	Artery and Veins
OD	Optical Disc

Chapter 1

Introduction

1.1 Introduction

The retinal vessel and optic disc are the only part of the human blood circulation system that can be observed in a non-invasive way directly. The analysis of biomedical images is one of the in-growth research fields. It is related to the study and analysis of digital images based on image processing techniques using computational tools that help in the analysis of clinical problem [1].

In the diagnosis of glaucoma, it is very important to detection of optical disc. The correct segmentation and detection of the optic disc from the retina is key for the detection of glaucoma. Recently, rapid progress in the field of biomedical image analysis research has proven to be significantly important, since it reduces the use of invasive approaches for diagnostic purposes. This proposal is based on the analysis of the fundus retinal images for the ocular disease diagnosis with the aid of computerized algorithms.

The blood vessel and optic disc of the retina can be used to diagnose different diseases related to the eyes, diabetic retinopathy, glaucoma and hypertension, etc. In addition, each individual has a different network of blood vessels, so it can also be used for biometric identification. The structure of the blood vessels of the retina is a very complex network and an efficient algorithm is required to detect it automatically.

DR is a disease of eye which cause the blindness. It is basically resultant of complicated diabetes mellitus and which damages the retinal vasculature. Patients become aware of this silent disease only when they have vision problems. However, the late diagnosis of this change can increase the chance of vision loss or can make the treatment more complex is complicated [2] .

There are two categories of DR, proliferative diabetic retinopathy (PDR) and Non-proliferative diabetic retinopathy (NPDR). DR is usually detected with the help of an eye exam that identifies patients with DR who is under the threat of that eye disease which need the essential treatment for the averting of vision loss [3]. The detection of diseases related to the eyes at an early stage has a great influence in the prevention of the loss of vision of the patient and in the increase of the quality of life [4].

1.2 Image Analysis

The process of obtaining valuable information from the digital images by using various methods are called image analysis. Image analysis acts an important role in various areas like remote sensing which provides the information about recognition of planetary resources, magnetic resonance imaging (MRI) for detection of cancer and tumor. Image analysis is used in diagnosing the disease. For this purpose, an efficient tool used to diagnose the disease automatically to prevent it from developing it in the early stages. This research work is focused on retinal images.

1.2.1 Retinal Fundus Imaging

In 1850, the tool for the analysis of retinal image was invented. Despite the fact that a translator's eye part is still needed for external inspection. The ophthalmologists examined the eye using Ophthalmoscopy, which provides information about retina and vitamin comic conditions. The ophthalmoscopy is used for the examination of the eye also called fundoscopy. It is based on the alignment of illuminated light and the point of observation. In fundoscopy special types of lens and mirrors are used which are placed between the eye of patient and physician. The standard acquisition protocol is used for the examination of eye. The head of the patient is placed in the front of the imaging device. The light is emitted into the eye by the spotlight

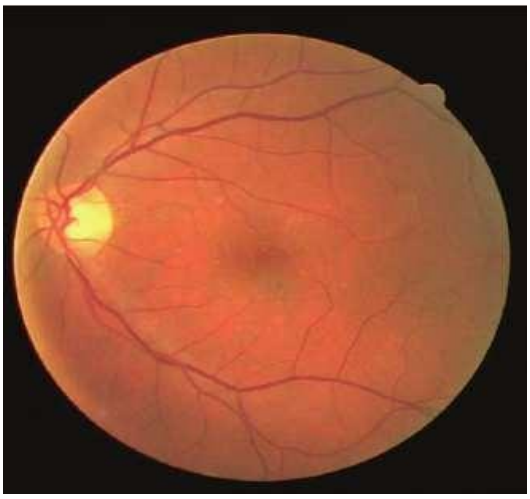

Figure 1.1: Retinal fundus image

in the environment of darkroom and the camera captures the reflected light. The ophthalmoscopes are of two types direct and indirect. The direct ophthalmoscope has small flash light and it has many lenses. The magnification of lenses is up to 15 times. The indirect ophthalmoscope is fixed on the headband and gives the broader view [5]. The internal surface image of the eye like posterior pole, retina macula and optical disc can be attained using fundus camera which presents the expanded view. The tropic amide medication is used to inspect the verge regions of the retina if needed. Generally undilation is used as sometimes dilation causes irritation to the patient. The low and high range of the image resolution of the imaging device is from 768×584 and 3504×2336 pixels respectively. Mostly high resolutions cameras are used which provides the fine detail about the vessels and the other structure. Fundus camera and the attained image is shown in Figure 1.1.

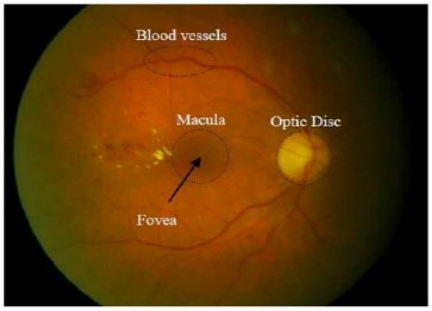

Figure 1.2: Optic disc and blood vessels

In [6], Abramoff et al. introduces the imaging modalities in fundus imaging including stereo fundus photography, hyperspectral imaging, fluorescein angiography (FA), scanning laser ophthalmoscope (SLO). In stereo fundus photography depth perception can be achieved. There can be two or more than two view angles of the retinal fundus image that can be acquired at the same time which helps in depth perception. In hyperspectral imaging the fundus camera can select the particular wavelength bands of the light along with the visible light.

FA is a type of image which gives the information of the photons that are emitted by the contrast agent like indocyanine green fluorophore or fluorescein and are injected in the bloodstream of the patient. SLO captures the image of the retina using low powered lasers. The light that reaches the surface of the retina is a moving narrow beam of light that can detour maximum ocular media opacities like corneal scars, vitreous hemorrhage cataracts and it can give the detail of the surface of the retina. Another imaging method is optical coherence tomography (OCT). This approach is used to capture 3D images and it is applicable near infrared light. The time of flight of the light deflected through the retina is measured using Michaelson interferometry technique. It has a benefit that it can penetrate into the scattering medium due to the long wavelength of light. It provides cross-sectional images of high resolution which helps in imaging the retina [7].This imaging approach is also used in cardiology and dermatology [5]. The downside of this modality is the time of acquisition it takes for attaining FOV which is greater as compared to the fundus camera and it has higher cost as well.

Fundus imaging is basically a process for examining the retina and diagnosing the retinal diseases like diabetic retinopathy [6] and Glaucoma. This process produces the digital retinal image. This technology is economical and widely used in the screening of different diseases. Also in fundus imaging data can be transferred easily from the network to the data server. There are other difficulties as well in the accurate segmentation like non-uniform illumination, contrast variation and noise.

1.2.1.1 Optic disc

OD which color is yellowish and its shape is oval resides as segment of retina. It is a point where optic nerve starts and retina gets the blood from blood vessels. The size of OD varies from person to person. It is called blind spot. It consists of two parts; optic cup (OC) and the neuroretinal rim. OC is a depression having variable size and is present in the center of the OD. This part of OD

helps in the diagnosis of Glaucoma as the increment in the size of OD leads to development of Glaucoma. The neuroretinal is the tissue between the OD and OC.

1.2.1.2 Retinal blood vessels

Retinal vessels is also known as vein and the arteries. It carries blood from and to the different parts of the eye. It helps in the diagnosis of different diseases like diabetic retinopathy.

1.2.1.3 Fovea

A part of eye that have no retinal blood vessels and small darkest area of retina is called fovea.

1.2.1.4 Macula

Macula is present in the center of the retina and its region is dark and pigmented. It has diameter of 5.5mm. It can absorb the excess of blue color and ultraviolet rays.

1.2.1.5 Problems in Retinal Fundus Imaging

Good quality of fundus image performs an eminent role for the diagnosis of the disease. In the fundus image, there can be artifacts that create problems in the correct recognition of the ailment. Following factors affects the image and makes the analysis a challenging problem.

- Noise
- Non-uniform illumination
- Inter-varying contrast
- Intra-varying contrast
- Pathologies

There are three types of noise include gaussian, speckle, pepper and salt noise which affects the retinal image. Gaussian noise caused by adding Gaussian distribution having fixed values with zero mean in the pixels of the image. Speckle noise is granulose in nature and reduces the quality of the image. Salt and pepper noise is present in the form of black and white spots randomly distributed on the image caused by ADC and bit errors. One of the common problems is non-uniform illumination caused by shading effects which reduce the effectiveness. The non-uniform illumination covers the OD and makes it difficult to detect the true boundary as in Figure 1.4. Intra-varying contrast is the variation of the contrast within the retinal fundus image shown in Figure 1.5. Inter-varying contrast is due to the variation of the contrast between different retinal fundus images with respect to one another shown in Figure 1.6. Pathologies have also negative impact, affect the retinal image and make it even more difficult to find the exact OD as in Figure 1.7. The photographer; camera and patient can also be responsible for a bad quality image. Special types of cameras are used for fundus photography including traditional office based, miniature tabletop, point and shoot off the shelf, integrated adapter based handheld and smartphone-based ophthalmic cameras. These cameras are used based on the requirements as these cameras have some limitation. Traditional office-based camera produces a good image but needs to be trained professional to run due to its complexity. The miniature tabletop camera is used in the clinical environment. The point and shoot off the shelf camera is low cost, but it is less focused. Integrated adapter-based camera gives high resolution, but it is time consuming because there is need to align the light beam

manually. The disadvantage of using mobile phone-based cameras is, it has low contrast and has narrow FOV as compared to other clinical fundus cameras. Besides this, a camera can also produce a poor image if a flash tube of the camera is not working properly, or there is timing issue i.e. in opening and closing of the shutter which changes the nature of the film chemically due to the light.

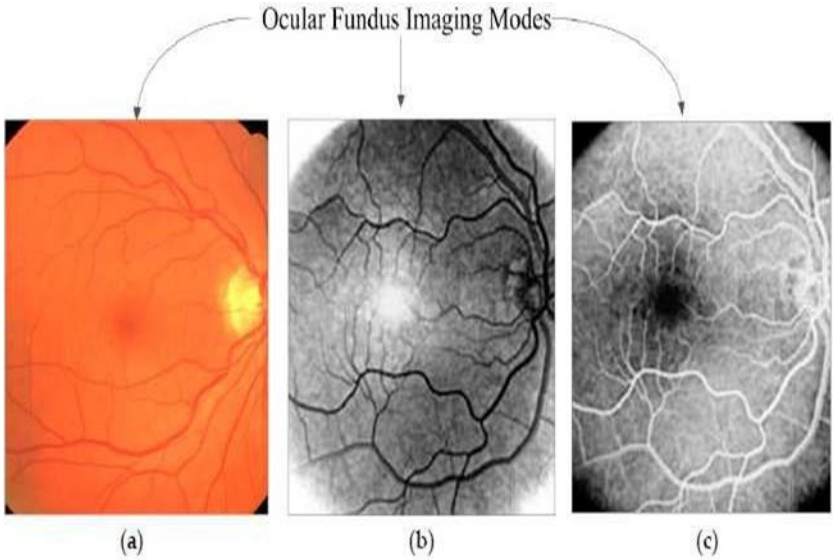

Figure 1.3: Imaging modes of ocular fundus photography a) Full color retinal fundus image; b) Monochromatic retinal fundus Image; c) Fluorescence angiogram retinal fundus image

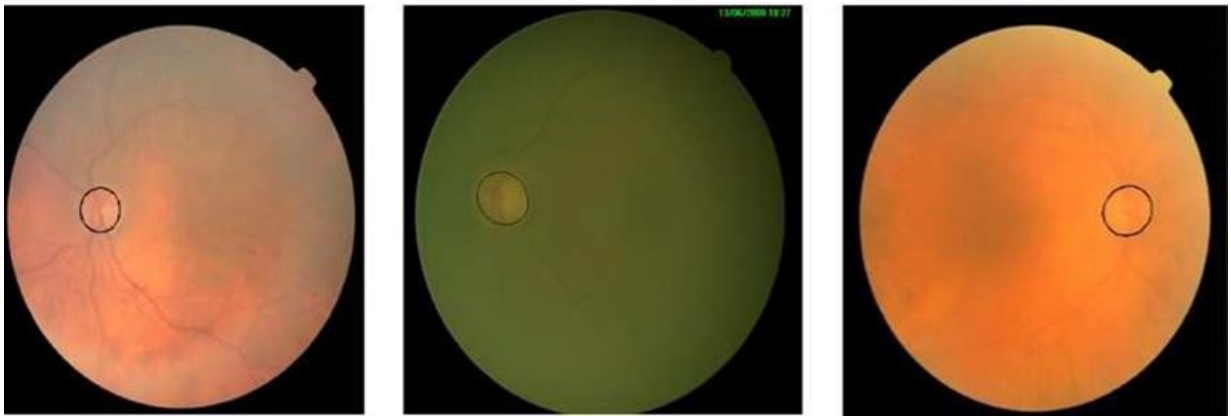

Figure 1.4: Detection of OD in nonuniform illumination

1.3 Structure of Eye

There are two parts of eye, i.e., anterior and the posterior compartments as shown in Figure 1.8. Furthermore, there are two groups i.e., internal and external that are present in the eye which consists of fibrous layers. The internal group consists of retina while the external comprises of cornea, sclera and the choroid. Moreover it has two parts the visual part which is called posteromedial and the non-visual portion, i.e., anterior. The visual part starts from fovea or macula and covers the ora serrata.

This research is based on retinal images. The retina is the most sensitive part of the eye. The diameter of the retina is about 22mm. It has tissues having thin sheet whose thickness is approximately 100-250. It lies in front of the choroid and behind the vitreous body. There is a thin layer of a cellular Bruch's membrane, whose thickness is about 2 to 4μm which separates the layer of choroid and the retina [8]. Retina is connected to the brain through the optic nerve [9]. It consists of tissues that is part of the nascent brain [10]. Any kind of damage either it is developmental or functional causes loss of vision. There are three layers of nerve cells in the structure of retina.

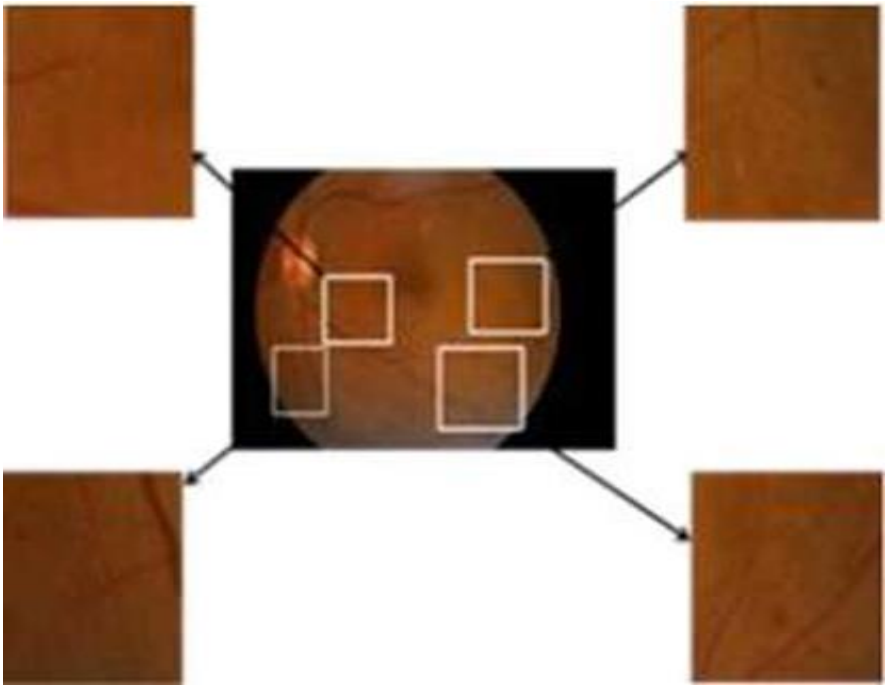

Figure 1.5: Intra varying contrast

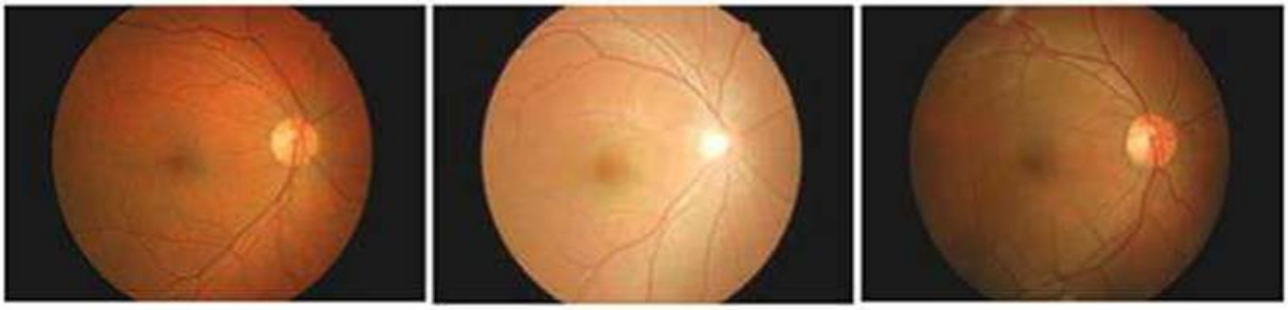

Figure 1.6: Inter varying contras

These three nerve cells has a separation by two layer having synapses that connects the cells from each other as shown in Figure 1.8. The retinal pigment epithelium (RPE) consists of melanin and it is the inmost layer. Melanin is a pigment which is black in color and absorbs the excess of light. There are receptors of light at the back side of retina which are close to the RPE and the neurons processes and transfer the visual information to the front side [9]. In fact there are ten different layers of cells in the retinal structure as shown in Figure 1.8. Using OCT several layers of retina can be seen [11]. Retina consists of photoreceptors that are light sensitive. These photoreceptors contain rods and cons. The rods produce scotopic vision while the cones produce photopic vision because cones are less light sensitive. The cones are accountable for the recognition of color and are able to perceive adequate detail. The amount of photoreceptors i.e. rods and cones varies in the retina. In the fovea, cones are present in greater number while the rods are dispersed and are absent.

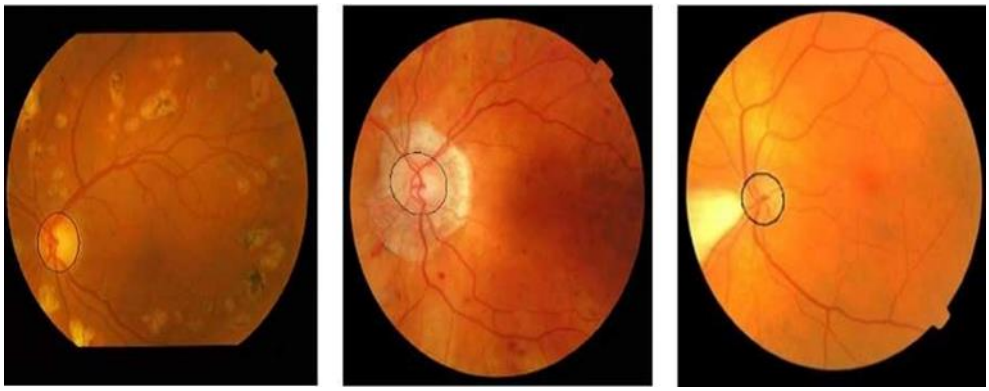

Figure 1.7: Detection of OD in pathologies

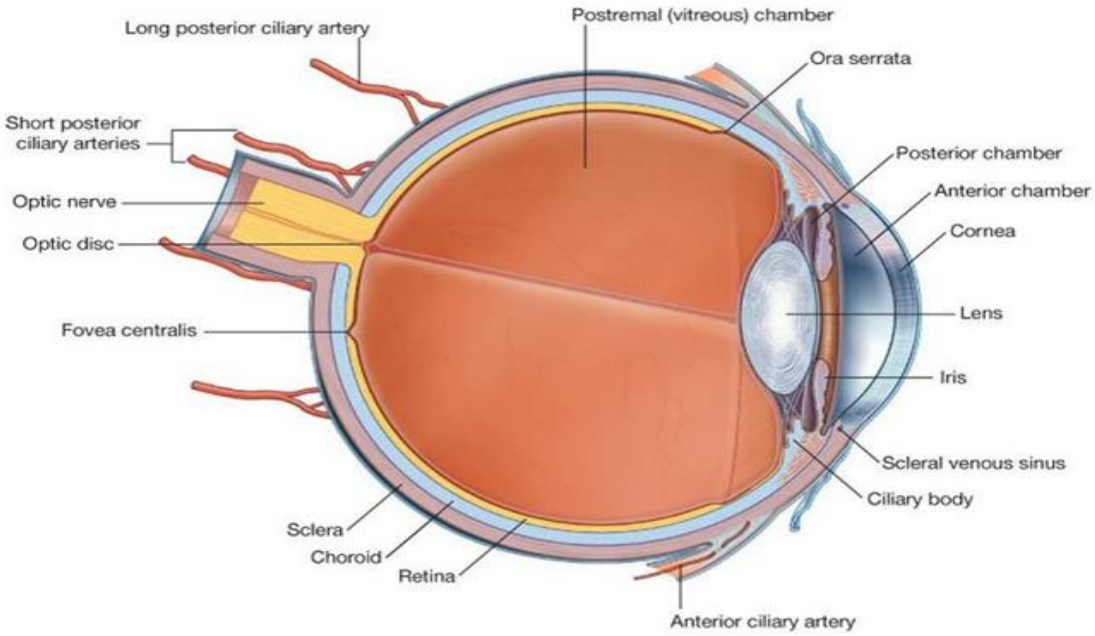

Figure 1.8: Structure of the eye

1.4 Glaucoma

Millions of people are affected by various retinal diseases. Depending on the nature of the disease some are curable while the rest leads to blindness. These diseases include Mascular degeneration, Diabetic retinopathy, Retinitis pigmentosa, Choroideremia, Glaucoma and many others. Among all, the most common disease is Diabetic retinopathy caused by increment of sugar level in blood. The most dangerous disease is Glaucoma which critically affects the optic nerve and has no symptoms. Optic nerve connects the optic chiasm with OD and it is 50mm long. OD consists of 1.2 million axons. Glaucoma is a retinal disease commonly caused by rise in intraocular pressure (IOP) and other causes include family history, migraines, high blood pressure and obesity. Sometimes it can be result of blocked blood vessels within the eye, eye infection and inflammatory conditions. It is second leading source of loss of vision. The loss of vision caused by Glaucoma leads to blindness. IOP is the pressure of the fluid inside the eye. It is formed in the ciliary body behind the iris. It passes through the pupil and flows out through the drainage channel called trabecular meshwork. This watery fluid exits the channel at an angle where cornea and iris meet. The IOP for a healthy eye is considered between 12-22mm Hg and above 22mm Hg, it shows the possibility of Glaucoma. It is expected that number of people affected by Glaucoma will be around 79.6 million by 2020 [12]. This disease damages the optic nerve. In retina there are millions of ganglion cells which are damaged due to this disease. Ganglion cells are neurons that receive and transfer the visual information to the brain. Once the ganglion cells are damaged, they are not repairable which makes this disease not curable. With the help of treatment its process of development can be lessen. The process of loss of vision caused by this disease is irreversible. Glaucoma disease is present around the OD. The CDR for healthy eye is 0.65 [13] and if this ratio increases then it shows

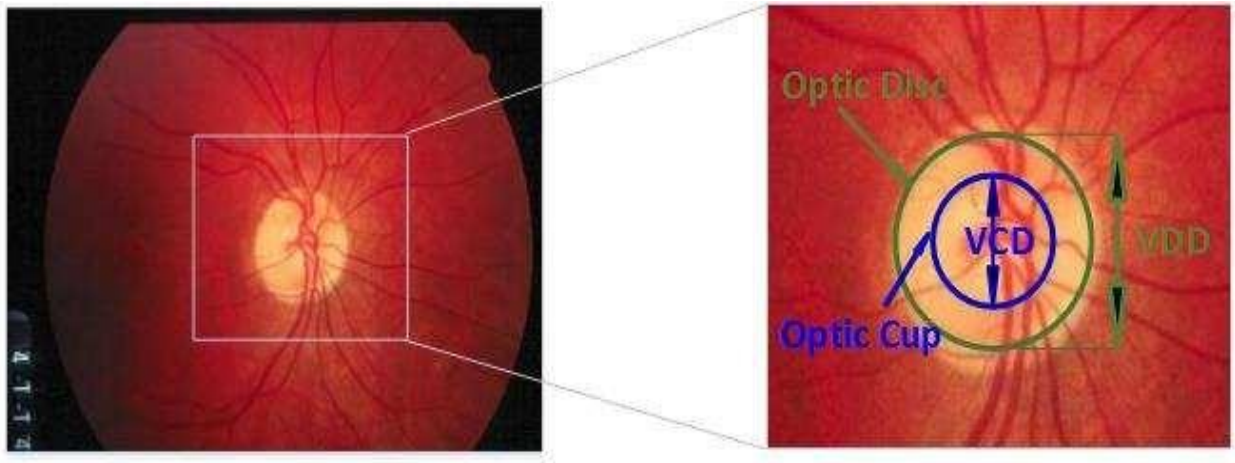

Figure 1.9: Optic disc and Optic cup

1.4.1 Types of Glaucoma

There are different types of kinds of Glaucoma

1.4.1.1 Open angle Glaucoma

In open angle Glaucoma fluid gets blocked inside the eye rises the IOP. In this type there is absence of other disorders, congenital irregularities and in which gonioscopy indicates that the anterior chamber angle is normal. It arises due to the loss of retinal ganglion cells and its visual field defects. It is also known as primary or chronic Glaucoma.

1.4.1.2 Angle closure Glaucoma

Angle closure Glaucoma originates due sudden rise in IOP. It arises due to the blockage of the drainage canals. In this case the angle between the iris and the cornea is very narrow therefore it is also known as narrow angle Glaucoma or acute Glaucoma.

1.4.1.3 Normal tension Glaucoma

Normal tension Glaucoma damages the ganglion cell without increasing the IOP. It is called normal pressure or low tension Glaucoma.

1.4.1.4 Congential Glaucoma

Congenital Glaucoma is inherited and mostly found in children.

1.5 Problem Description

Glaucoma is lead to blindness and irreversible. This disease has no symptoms and its early diagnosis is essential for treatment to slow down its progression. The background photograph is used to take the image of the retina. The main challenge is to achieve the correct segmentation of blood vessels and optical disc from the image of the retina. The optical disc and blood vessels segmentation provides information about the position, shape and size, and also shows if there is any abnormal growth in any specific part of the eye. Which make the segmentation a challenging problem including?

- Variation in the shape of the object
- Variation in the quality of the image
- Non uniform illumination
- Noise

To deal with all these problems, it is necessary to perform preprocessing and post-processing techniques together with segmentation, which takes time and makes the processing slow. The process of blood vessels and optical disc segmentation requires several processing techniques that increase latency. For efficient detection and segmentation and to avoid preprocessing and post processing steps, a framework that minimizes latency and increases performance is required. Glaucoma can be diagnosed by CDR and intraocular pressure (IOP). The measurement of intraocular pressure is not always the correct way to diagnose glaucoma, since this disease sometimes comes out with normal intraocular pressure.

1.6 Discussion to Proposed Solution

In order to deal all the issues described in Section 1.5 and to save pre-processing cost, the learning-based approaches can perform better based on trained knowledge. The Semantic segmentation is the most recent form of learning-based methods which deal with segmentation task by deep learning of the valuable features from the image. So, to perform the segmentation with noisy retinal images semantic segmentation can be a powerful tool.

1.6.1 Introduction to semantic segmentation and segmentation networks

The CNNs are famous for image classification task with accuracy based on learned knowledge during intensive training. The pixel wise classification is also a form of classification the only differences is that the classification network just classify the image with birds eye view depending upon the relevant features and assign a class to the image, whereas the semantic segmentation classify each pixel of the image and assign the class label to this pixel. The process of assigning the label to each pixel is performed in one instance, that make the semantic segmentation network perform faster as compared to other local feature-based methods.

In other words, semantic segmentation algorithms are used to solve structured pixel-wise classification problems based on CNN, in which all the pixel in the images are classified through the network and assigned with a candidate class. They obtain a coarse label map from the network by classifying every local region in image, and bus, car, train, boat and bicycle person. Limitations of semantic segmentation algorithms is that it depends upon the pixel label to get trained, the pixel label is also an image with different pixel values for each class in the image [14].

For pixel wise semantic segmentation SegNet is used. It has an ability to understand the spatial relationship like context and shapes like road, building. Most of the pixels belong to large class. It reduce the size of image and segment the required region [15].

Considering the famous semantic segmentation networks , fully convolutional networks (FCNs) are familiar for the semantic segmentation using famous deep learning networks AlexNet [16], VGG net and GoogLeNet [17], VGG net, and GoogLeNet to create FCN-AlexNet, FCN-VGGnet, FCN-GoogLeNet. The pixel prediction layer assigns the pixel labels and create the output with same size. The Figure shows the schematic of FCN in which the network layers are shown with output prediction.

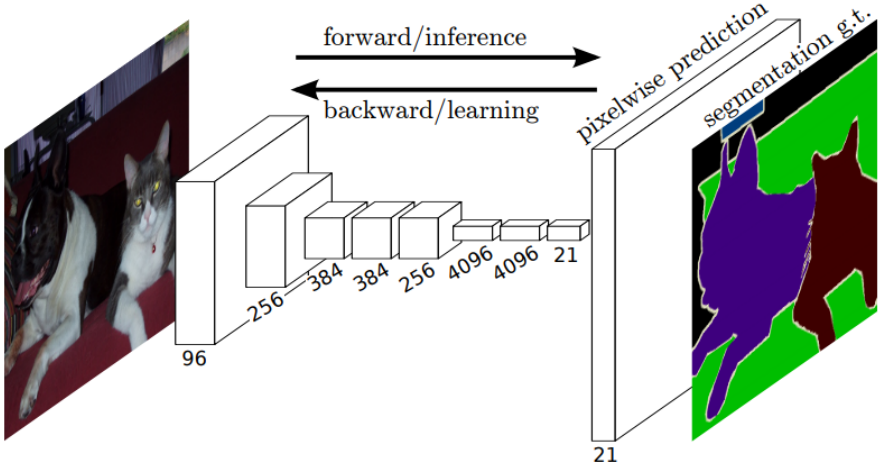

Figure 1.10: The FCN schematic for the dense per pixel prediction [18]

The other more famous semantic segmentation architecture is known as SegNet [15]. Unlike FCN the SegNet is an encoder decoder architecture in which fully connected layers are not used, where fully connected layer consumes much trainable parameters that can make the task computationally expensive. In SegNet the VGG-16 [16] network is used as backbone where the decoder is the mirror copy of the encoder. The SegNet encoder-decoder network schematic is shown in the Figure 1.12. SegNet is basically used for multi-class road scene segmentation of the CamVid dataset [19] on which SegNet is basically used, the number of classes were 11 like trees, car, buildings, road, sky etc. In case of using the SegNet for two classes the pixel labels can be 0 or 1. The more explanation to the SegNet is available in the Chapter 3.

Considering all the fully convolutional networks for the semantic segmentation, the training image with corresponding ground truth images are required to train the network. Also the performance of the segmentation is much dependent on the amount of training images and variation of the features.

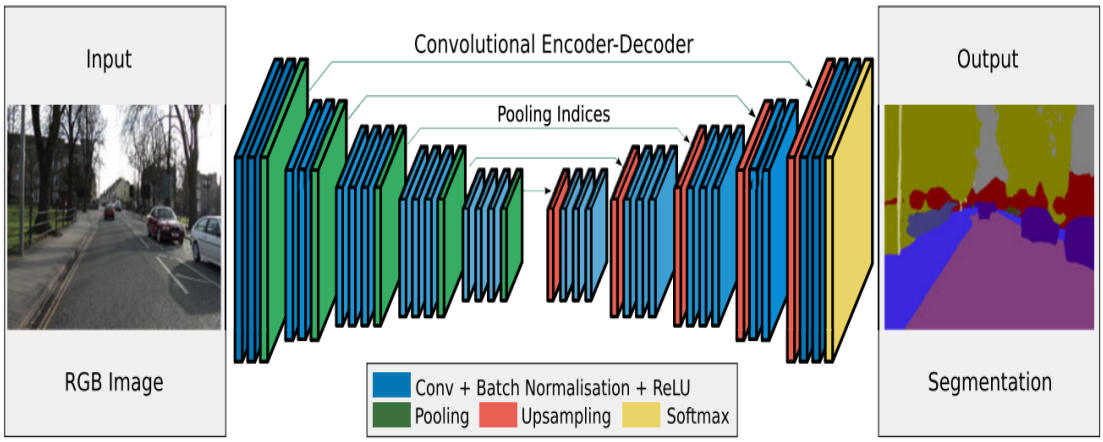

Figure 1.11: Semantic Segmentation

1.7 Main Contributions

Following are the major contributions and the advantages of the scheme:

- This technique will use the original image without the prior pre-processing.
- This scheme is learning based so no conventional image processing schemes will be used for the training of the network.
- Unlike the traditional image processing schemes per-image processing time will be reduced to less than a second.
- The method will provide good accuracy even with inferior quality images.

1.8 Thesis Overview

Thesis follows the following chapters:

Chapter2: It explains basics of deep learning. There are different state of the art techniques which have been discussed in this chapter are based on the convolutional neural network.

Chapter3: It describes the methodology of segmentation of vessels and OD based on CNN.

Chapter 4: This chapter presented the experimental results that we have used are MESSIDOR for optical disc segmentation and DRIVE for vessels segmentation. The result shows accuracy, sensitivity, specificity.

Chapter5: This chapter comprises of conclusion and perspective of the proposed method.

Chapter 2

Literature Review

Presently, developing an automatic system for screening a large number of patients with sight threatening diseases like DR and providing an automated detection of the disease is the focus of researchers. Image processing is the most suitable tool for screening DR, where the acquired digital images are evaluated by automated systems for analysis purposes. Fundus image analysis is a difficult task as fundus images vary in terms of color or gray levels, this is due to the fact that the morphology of retinal structures and the presence of specific features in various patients may lead to incorrect results. There have been few research surveys that detect retinal parts like optic disk, blood vessels, FOV and retinal lesions containing exudates, micro-aneurysms and hemorrhages [5]-[21].

2.1 Introduction

Presently, developing an automatic system for screening a large number of patients with sight threatening diseases like DR and providing an automated detection of the disease is the focus of researchers. Image processing is the most suitable tool for screening DR, where the acquired digital images are evaluated by automated systems for analysis purposes. Fundus image analysis is a difficult task as fundus images vary in terms of color or gray levels, this is due to the fact that the morphology of retinal structures and the presence of specific features in various patients may lead to incorrect results. There have been few research surveys that detect retinal parts like optic disk, blood vessels, FOV and retinal lesions containing exudates, micro-aneurysms and hemorrhages [20]-[21]. Diabetic retinopathy is a common disease which cause of blindness.

Akram et al. proposed, segmentation method of optical disc using Hough transform and multilayered thresholding techniques and blood vessels and grading of proliferative diabetic retinopathy using multivariate m-Mediods based classifier where, the system extracts the vascular pattern [22]. Akber et al. presented an automatic method which segment the HR using papilledema and arteriovenous ratio in retinal image. First for A/V classification using SVM and RBF to classify the arteriovenous ratio. Secondly, a system which evaluation of optic nerve head (ONH) for papilledema is proposed [23]. Kurniawan et al. represented the automatic method which segment the HR using papilledema and arteriovenous ratio in retinal image [24]. Fatima et al. proposed a simple and efficient method to automatically detect papilledema through fundus images by SVM aided by preprocessing, in details, 13 features are extracted from STARE dataset which are helpful in detecting this disease and combined to form a feature set where the final prediction is made by SVM classifier, where overall method gives an accuracy of 96.67% [25]. Yousaf et al. classified the images into normal and diseased images, they used a classifier of SVM, and RBF kernel is used for classification of image. Accuracy of this classifier is achieved 95.65% [26].

Estrada et al. proposed an underlying vessel topology to better classify small and midsized vessels that are present in the fundus image [27]. Relan et al. described a technique which use the color features of A/V in a Gaussian mixture model to successfully classify the vessels of retinal an

expectation maximization (GMM-EM) unsupervised classifier [30]. Niemeijer proposed an automated method to estimate the AVR in retinal color images by detecting the location of the optic disc, determining an appropriate region of interest (ROI), classifying vessels as arteries or veins, estimating vessel widths, and calculating the AVR [31].

Muramatsu et al. proposed a method which is related to vessel detection algorithm, the method deals with total 20 cases, every case used for training and testing, where double ring filter and black top-hat transformation is used to identify blood vessels using the features are extracted from discriminant analysis [32]. Xu et al. worked in supervised method to classification of A/V in retinal image. To minimize the variations in feature space they used the inter subject normalization and intra image regularization method, the distinguishing characteristics of A/V novel features (first order) and texture features (second order) are employed [33]. Pachiyappan et al. detected and diagnosed glaucoma and diabetic retinopathy using OCT images through image processing techniques and morphological operations like histogram equalization, segmentation through the set of filters and threshold values [34]. Jestin et al. find out the retinal vessels by using graph cut method where the information from retina vessels is then used to estimate the location of the optical disk and then an AAN classifier is used which robotically classifies the disease in retinal image [35]. Acharya et al. proposed a computer-based classification of eye diseases using three different type of classifier, Fuzzy classifier, Neuro-Fuzzy classifier and ANN (Artificial Neural Network) and preprocessing image, they used dataset of 135 subjects that are fed to these classifiers after feature extraction [21]. Oliveira et al. presented a technique which merges the multiscale analysis. Multiscale FCNN of stationary wavelet transform to handle the retina vessel structure in terms of changing the width and their direction [36]. Bhuiyan et al. gave the idea for the classification of A/V by using color intensity and vessels crossover. In this technique extract the vascular network and classify vessels. Extraction of retinal vascular network by using deep learning based algorithm [21]. Li et al. presented novel method to segmentation of retinal vessel in supervised classification. Deep learning makes their method perfect to resolve the segmentation of retinal vessel as well as improved the loss function [36].

2.2 Background

Retina of the eye is affected when tiny blood vessels are damaged due to hypertension and high sugar level that results in vision loss problems. World Health Organization (WHO) predicts that over the next 25 years the number of people with diabetes will increase from 130 million to 350 million [37]. Computerized extraction of retinal vessels was improved using three novel operations by Soomro et al. [38].

Soomro et al. [39] proposed a method which based on deep learning. It along with pre-processing and post-processing. The issue of uneven illumination is handle by pre-processing. Fully convolutional network is designed and train it get the blood vessels. Background noise pixels are removed by using post-processing. This method is used to detect the tiny blood vessles and gives the good segmented image. Extraction of computerized retinal vessel was improved by two contrast-sensitive measures suggested by A.U. Khan et al. [37].

2.2.1 Vessel Tracking

The tracking methods try to find an unbroken blood vessel fragment, beginning from a given point which is selected automatically or manually, based on certain local information.

Soomro et al. proposed method of deep learning which was dependent on convolutional neural network (CNN) using dice loss function to segment the vessels of retinal images. They used colored images of retinal for their proposed method. They performed preprocessing steps for making procedure for accurate and to skip the uneven illumination of the images. They take CNN of a variational auto-encoder (VAE) but for their work. They updated it into U-Net. They generated output of segmented vessels with no change effect in resolution of retinal images. After experiment their results revealed good performance against old methods [40]. Tolias et al. [33] represent a method for detect the blood vessels in fundus images by using morphological descriptions. They used the C-means clustering algorithm. Chutatape et al. [35] represent an algorithm that detect the blood vessel using second order derivative Gaussian matched filter along with Kalman Filter in ocular fundus images.

2.2.2 OD Segmentation

Optical segmentation is the most important step in diagnosis for treatment of Glaucoma. Find a correct CDR it gives the information of Glaucoma, it's possible if we make accurate the segmentation of optical disc. Supervised and unsupervised methods have been used. There are many common approaches deformable part model, circular Hough transform, pixel and super pixel techniques and morphological methods. C. Muramatsu et al. [41], Proposed a method circular Hough transform (CHT) is used to track optical disc according to good computational effect. J. Cheng et al. [42] Optical disc is an elliptical in shape. They used elliptical Hough transform to detect an OD. Cheng et al. proposed a technique for the segmentation of OC and OD. This method was based on super pixel classification [37].

Rehman et al. [43] proposed a method to detect the optic disk detection and localization for retinal fundus images. For optical localization they used morphological process that is followed by circular Hough transform (CHT). They used texture and region based statistical features. They used the highly discriminative feature and four classifier. They used the RF based classifier which have the excellent performance. Zahoor et al. [44] proposed a method to obtain of region of interest (ROI) and adaptive thresholding based novel polar transform. They used a good technique optical disc is segmented and localized in fast and accurate way. This methodology is apply publically available dataset on MESSIODR, DRIONS etc.

Fan et al. [45] proposed structured learning based an algorithm. In this paper they trained a classifier which detect the edge map of optical. After obtaining the edge map thresholding is applied. Circular Hough transform is used to extract the boundary of optical disc.

Morales et al. [46] Proposed a method based on mathematically morphology besides principal component analysis (PCA). They used different operations like generalized distance function (GDF), stochastic watershed and geodesic transformations. Abdullah et al. [47] represents an algorithm that based on CHT and morphological operations. Optical disc is enhanced by using morphological operators to eliminate the pathologies and retinal vasculature.

2.2 Summary

Different techniques of vessels detection have been discussed in this chapter. It is concluded from the literature that the pre-processing (normalization and image enhancement) is an essential part in vessel detection. Optic disk detection can be used for vessel detection. Previously it is used for glaucoma screening but not applied in contrast compensation. To extract true vessels, it is essential to detect optic disk correctly. There are two factors in Optic detection that play a vital role. If we apply a contrast normalization on an image having optic disk in it, the normalization will not be performed well because of uneven illumination and some small vessels may be lost. As there are vessels inside optic disk region and if optic disk is not compensated then the false vessels will be created on the boundary of OD. So, OD detection and its compensation is the most essential step for image normalization and vessel detection.

Chapter 3

Methodology

3.1 Proposed Method

Segmentation task, the actual image is provided to SegNet without prior pre-processing. The SegNet takes the input data for training and at the test phase the test image is provided to the network which provide the segmentation mask as shown in the Figure 3.1, as the provided mask from the SegNet is bit dilated so post processing is applied to refine the segmentation of the blood vessels.

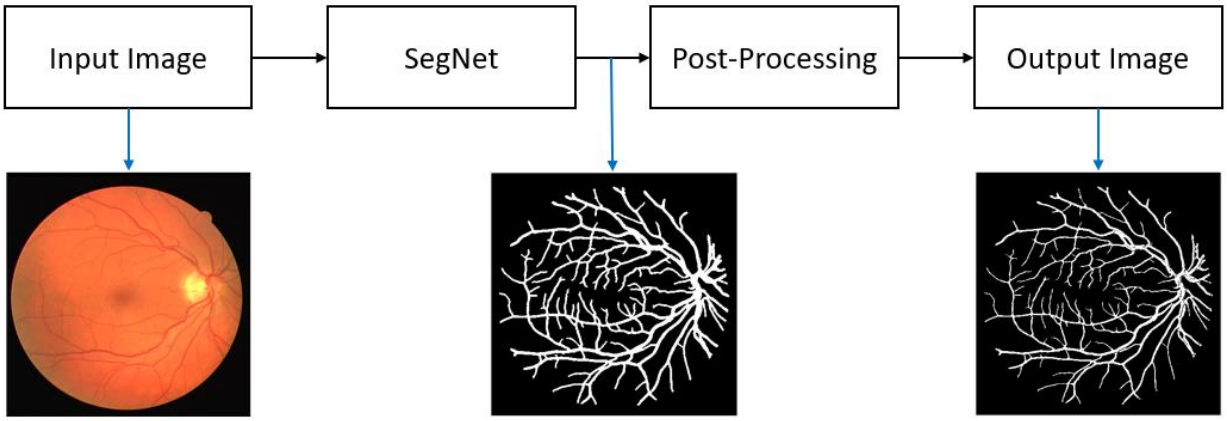

Figure 3.1: Vessels segmentation over all process

3.2 SegNet for Vessel/OD Segmentation

SegNet have multiple layers in the form of encoder and decoder. Encoder apply convolution, Relu, batch normalization, non-linearity and max pooling on result. Index of value is extracted from each window. Decoder don't have a non-linearity it is same like encoders. It upsamples the image and using indices stored at this stage. Output of this decoder is given to a softmax classifier and take last prediction. The output will be an n channel image, it convert into RGB image. So quality of output is good. The SegNet is straight forward design in which the decoder is exactly the mirror copy of encoder with same number of layers, the only difference is the encoder just down-samples the image in order to represent it buy the minor features, where the decoder apply the up-sampling operations with loss function and the pixel classification layer in the end.

As described earlier the SegNet is basically used for the road scene segmentation for the 11 classes. In order to use the SegNet for two classes few changes into the network is required. Considering the DRIVE dataset for vessel segmentation the 447 × 447 image size is used in our experiment so to use the SegNet for this image size, input image layer is changed according to our input size and the related connection to next layers are made. Secondly the last convolution layer at the decoder side is related with the number of classes to be segment, so in order to use the SegNet for binary

classes like OD/ Non-OD or Vessel/ Non-Vessel the filter size of the last convolutional layer in the decoder is set to “2” for the binary class.

As mentioned earlier in order to segment the vessels or optical disc from the background the original image is provide to the SegNet and it provides the segmentation mask as the result. The figure below represents overall workflow for the vessel/OD segmentation.

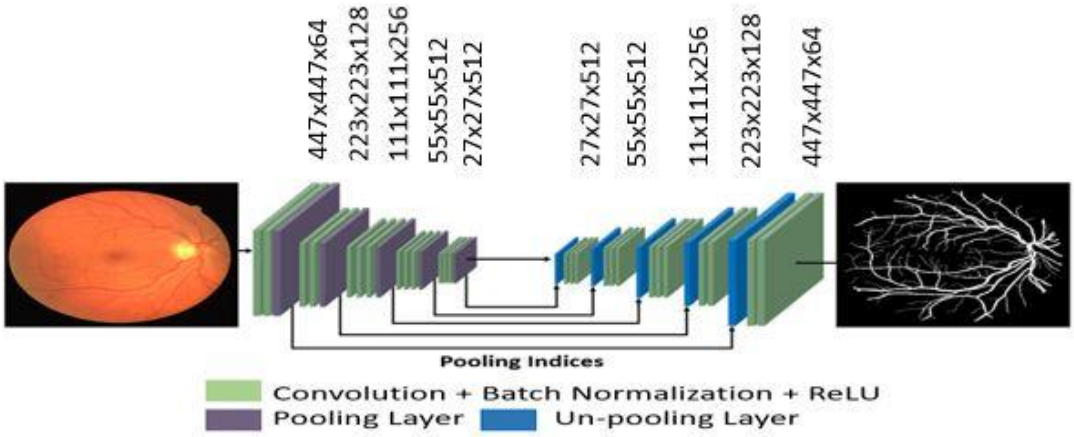

Figure 3.2: Vessels segmentation

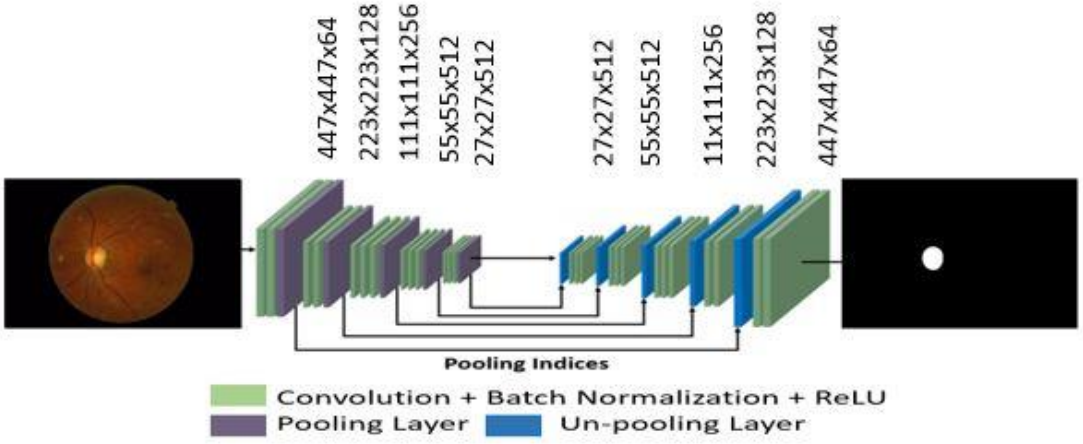

Figure 3.3: OD segmentation

3.2.1 Encoder Phase

SegNet is a FCNN which is used for semantic segmentation to classify each pixel available in the image (it is basically pixel wise segmentation). The pixel wise segmentation is the pixel wise classification in which each pixel is assigned with a label. The SegNet is based on VGG-16 structure in which 13 convolutional layers are used in encoder as shown in figure 3.4. All the convolutional layers are in combination with batch normalization layer and ReLU layer. In order to design the SegNet encoder the fully connected layers of VGG-16 are removed and the down-sampled image from the encoder is directly provided to the decoder for up-sampling. Where after each convolutional block in decoder a max pooling layer is used to reduce the feature map size, these pooling layers provide the pooling indices to the decoder as shown in Figure 3.2 and 3.3.

Table 1: Layer wise feature map activation for proposed network

Name	Type	Channel/Filter Size	Output	Learnable Parameter
Input	Image Input Layer		447x 447x3	0
Conv1_1	Convolution layer	64/3x3	447x447x64	1792
Bn_conv1_1	Batch Normalization		447x447x 64	128
Relu1_1	ReLU		447x447x64	0
Conv1_2	Convolution layer	64/3x3	447x447x64	36928
Bn_conv1_2	Batch Normalization		447x447x64	128
Relu1_2	ReLu		447x447x64	0
Pool1	Max pooling	223x223x64		0
Conv2_1	Convolution layer	128/3x3	223x223x128	73856
Bn_conv2_	Batch Normalization		223x223x128	256
Relu2_1	ReLU		223x223x128	0
Conv2_2	Convolution layer	128/3x3	223x223x128	147584
Bn_conv2_2	Batch Normalization		223x 223x128	256
Relu2_2	ReLU		223x223x128	0
Pool2	Max Pooling	111x111x128		0

Conv3_1	Convolution layer	256/3x3	111x111x256	295168
Bn_conv3_1	Batch Normalization		111x111x256	512
Relu3_1	ReLU		111x111x256	0
Conv3_2	Convolution layer	256/3x3	111x111x256	590080
Bn_conv3_2	Batch Normalization		111x111x256	512
Relu3_2	ReLU		111x111x256	0
Conv3_3	Convolution layer	256/3x3	111x111x256	590080
Bn_conv3_3	Batch Normalization		111x111x256	512
Relu3_3	ReLU		111x111x256	0
Pool3	Max Pooling		55x55x256	0
Conv4_1	Convolution layer	512/3x3	55x55x512	1180160
Bn_conv4_1	Batch Normalization		55x55x512	1024
Relu4_1	ReLU		55x55x512	0
Conv4_2	Convolution layer	512/3x3	55x55x512	2359808
Bn_conv4_2	Batch Normalization		55x55x512	1024
Relu4_2	ReLU		55x55x512	0
Conv4_3	Convolution layer	512/3x3	55x55x512	2359808
Bn_conv4_3	Batch Normalization		55x55x512	1024
Relu4_3	ReLU		55x55x512	0
Pool4	Max Pooling		27x27x512	0
Conv5_1	Convolution layer	512/3x3	27x27x512	2359808
Bn_conv5_1	Batch Normalization		27x27x512	1024
Relu5_1	ReLU		27x27x512	0
Conv5_2	Convolution layer	512/3x3	27x27x512	2359808
Bn_conv5_2	Batch Normalization		27x27x512	1024
Relu5_2	ReLU		27x27x512	0
Conv5_3	Convolution layer	512/3x3	27x27x512	2359808

Bn_conv5_3	Batch Normalization		27x27x512	1024
Relu5_3	ReLU		27x27x512	0
Pool5	Max Pooling		13x13x512	0

3.2.1.1 Convolution

Convolutional neural network is an algorithm of deep learning. It takes an input image and assign the learnable weight and differentiate one from the other. In ConvNet preprocessing is not required related to different classification algorithm. While in basic methods filters are self-designed, with optimum training, ConvNets have the capability to learn these filters. A convolutional layer includes the parameters of filters which are learnable. The weight and height of the filters are smaller as compared to input volume. All of the filters are convolved with the i/p size to process an activation map made of neurons. Filter is slide around the height and width of input and to find dot products and filters are processed at every spatial position. The activation map along the depth dimension provide the o/p size of the convolutional layer. The height and width of filter is designed smaller than the output. All of the neurons are only related to a limited area of i/p size [22] where the receptive fields of the cells are small. The convolutional layers are connected and allow the filter of network to be learn, a pixel is correlated to the close pixels than to the farway pixels.

3.2.1.2 Pooling layer

The previous layers are helpful in order to minimize the size of image. It is just like shrinking an image to reduce the size of pixel. It cause to reduce the computational power. It is very helpful to extract the discriminative features, so training model is very effective and useful.

Maximum pooling layer takes the maximum values from the part of image which is covered by kernel. Average pooling layer takes average values from the part of the image which is covered by image. These layer have a capability to capture the low level details from the image.

.

3.2.1.3 ReLU layer

ReLU function is a bit wise linear function that give output is one if it is positive otherwise the output will be zero. ReLU function has become by default activation function for neural networks. The network model is easy to train and achieve best performance. The network of rectifier function is used for hidden layer are mentioned as rectified network.

3.2.1.4 Batch normalization

Batch normalization is a method for improving the stability and performance of neural network. It speeds up the learning process of a neural network, also the batch normalization enable the convolutional neural network to improve its learning because this layer itself learn a little bit more independently during the training procedure. It makes the architecture of deep learning is more effective and sophisticated because it prevents the activations to get too high or too low. The batch normalization is also helpful to reduce the phenomena of overfitting because of it regularization effects. The input of each layer that mean output of activation function is zero and standard

deviation is one. It's called "batch" normalization because during training, we normalized the activations of the previous layer for each batch, i.e. apply a transformation that maintains the mean activation close to 0 and the activation standard deviation close to 1.

3.2.2 Decoder Phase

The reverse process of encoder is called decoder. There are 13 convolutional layers used in mirror fashion as shown in figure 3.4. The pooling indices gives to the unpooling layer from the encoder pooling layers. Decoder uses the pooling indices which includes the information of location, image size and upsamples the image back to its original size. This image provides the softmax for loss calculation.

Table 2: Layer wise feature map activation for proposed network

Name	Type	Channel/Filter Size	Output	Learnable Parameter
Decoder5_unpool	Max Unpooling Layer		27x27x512	0
Decoder5_conv3	Convolution layer	512/3x3	27x27x512	2359808
Decoder5_bn_3	Batch Normalization		27x27x512	1024
Decoder5_relu_3	ReLU		27x27x512	0
Decoder5_Conv2	Convolution layer	512/3x3	27x27x512	2359808
Decoder5_bn_2	Batch Normalization		27x27x512	1024
Decoder5_relu_2	ReLu		27x27x512	0
Decoder5_conv1	Convolution layer	512/3x3	27x27x512	2359808
Decoder5_bn_1	Batch Normalization		27x27x512	1024
Decoder5_relu_1	ReLu		27x27x512	0
Decoder4_unpool	Max Unpooling		55x55x512	0
Decoder4_Conv3	Convolution layer	512/3x3	55x55x512	235988
Decoder4_bn_3	Batch Normalization		55x55x512	1024
Decoder4_relu_3	ReLU		55x55x512	0
Decoder4_Conv2	Convolution layer	512/3x3	55x55x512	2359808
Decoder4_bn_2	Batch Normalization		55x55x512	1024
Decoder4_relu_2	ReLU		55x55x512	0
Decoder4_Conv1	Convolution layer	256/3x3	55x55x256	1179904
Decoder4_bn_1	Batch Normalization		55x55x512	512

Decoder4_relu_1	ReLU		55x55x512	0
Decoder3_unpool	Max Pooling layer		111x111x256	0
Decoder3_Conv3	Convolution layer	256/3x3	111x111x256	590080
Decoder3_bn_3	Batch Normalization		111x111x256	512
Decoder3_relu_3	ReLU		111x111x256	0
Decoder3_Conv2	Convolution layer	256/3x3	111x111x256	590080
Decoder3_bn_2	Batch normalization		111x111x256	512
Decoder3_relu_2	ReLU		111x111x256	0
Decoder3_Conv1	Convolution layer	128/3x3	111x111x128	295040
Decoder3_bn_1	Batch Normalization		111x111x128	256
Decoder3_relu_1	ReLU		111x111x128	0
Decoder2_Unpool	Max pooling		223x223x128	0
Decoder2_Conv2	Convolution layer	128/3x3	223x223x128	147584
Decoder2_bn_2	Batch Normalization		223x223x128	256
Decoder2_relu_2	ReLU		223x223x128	0
Decoder2_Conv1	Convolution layer	64/3x3	223x223x64	73792
Decoder2_bn_1	Batch Normalization		223x223x64	128
Decoder2_relu_1	ReLU		223x223x64	0
Decoder1_Unpool	Max Pooling		447x447x64	0
Decoder1_Conv2	Convolution layer	64/3x3	447x447x64	36928
Decoder1_bn_2	Batch Normalization		447x447x64	128
Decoder1_relu_2	ReLU		447x447x64	0
Decoder1_Conv1	Convolution layer	2/3x3	447x447x2	1154
Decoder1_bn_1	Batch Normalization		447x447x2	4
Decoder1_relu_1	ReLU		447x447x2	0
Softmax	softmax		447x447x2	0
Labels	Max Pooling			0

3.2.2.1 Unpooling

The operation of pooling layer is non-invertible. We acquire an estimated inverse of the maxima within each pooling area in a set of switch variables. In deconvnet, the operation of unpooling layers are used the switches to place the reforms from the layer into proper positions. Basically the process of unpooling is associated with the semantic segmentation, in which the small sized feature maps are get bigger with the help of unpooling depending upon the window size for the upsampling process.

3.2.2.2 Loss function and pixel classification

In the final step the loss is calculated over the classes using the softmax loss function. Give the class label to each pixel in pixel classification layer by using loss function. The output of the network is a binary mask which represents the desired class with binary values.

3.2.3 Training of the proposed network

For training purpose of network for the semantic segmentation of the vessels/ OD successfully, huge amount of the data is required to provide the distinctive features to get trained. As the retinal images in the DRIVE dataset training are just 20 so it is very difficult to train a deep network with small number of images. The data augmentation is the technique that can be used to artificially increase the amount of data with distinctive features for the training. In our experiments the data augmentation with image translation, mirroring, rotations are used, and several images are created after resizing the image accordingly. In case of semantic segmentation the both image and the label are transformed to create the new artificial data. In this study the 2000 artificial images are made from the 20 images by the said transformations which are enough to train the semantic segmentation network.

In order to train the SegNet for vessel/OD segmentation a flat learning rate of 0.001 is used with the mini-batch size of 5, where the SGD is selected as the optimizer with momentum of 0.9 and we trained 10 epochs with the flat learning rate. As per the experimental observation as the network is not using any other connections that can empower the features traveling through the network so the continuous convolution degrades the image, and in this situation if we train it with high number of epochs the information loss is much. In result the 10 epochs training provides the handsome results for the segmentation using SegNet.

The output of the network are two binary mask images for both classes, the output images is then post-processed in order to refine the segmentation.

3.2.4 Dealing with the class imbalance

Considering the example images provided in Figure 3.4, it can be easily observed by the naked eye there is a huge difference between the number of pixels of vessel and non-vessel class. The vessel pixels are much smaller in the number as compared to the non-vessel pixels, the difference in pixel frequency is also shown in Figure 3.5. So, with this class imbalance in the training data

can create trouble during the training of the network in terms of accuracy of the system. The class imbalance will force the network train with the dominant class which is non-vessel class in this case. In order to deal with this problem frequency balancing is used which is similarly used in [15] for 11 classes. The median frequency balancing is used to deal class imbalance, which computes the weights of classes and the weights are added into the pixel classification layer to compensate the class imbalance.

Figure 3.4 Example image by DRIVE dataset

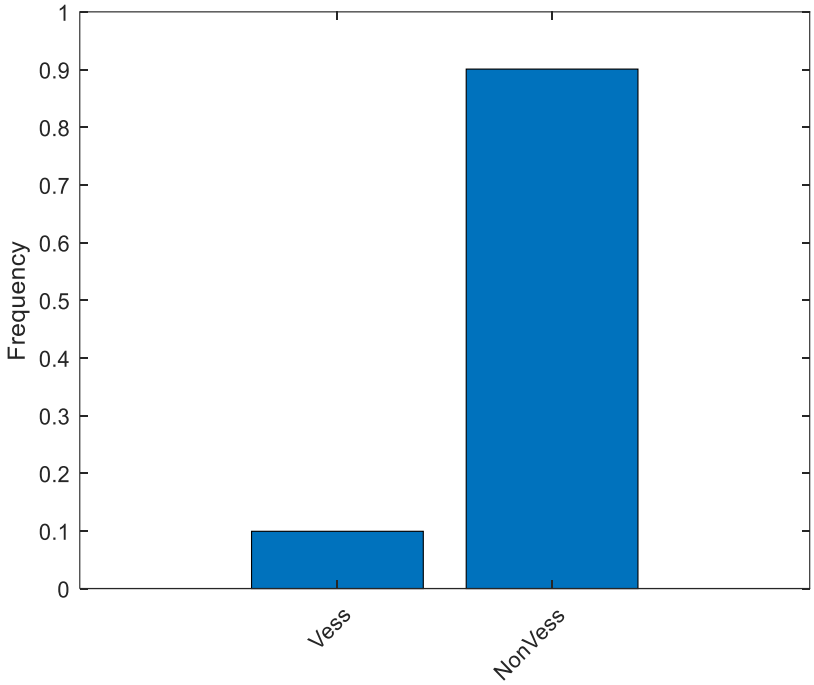

Figure 3.5 Difference in the pixel occurrence frequency in vessel and non-vessel classes

3.2.5 Post processing

The output of the SegNet is a binary mask which represent the 1 for vessel/OD pixel, whereas 0 for the background pixels. It can be seen from the Figure 3.2 when testing the image, the output of the SegNet is bit dilated, in order to make the boundary finer the post processing is required. To shrink the output mask the morphological erosion is used. As shown in the Figure 3.6 the morphological erosion is shrinking the vascular boundary. In our experiment the disc with radius 1 is chosen as the structuring element for the morphological operation.

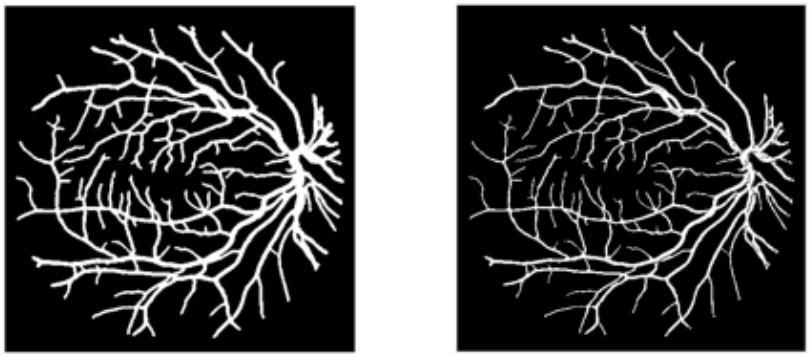

Figure 3.6: Post processing operation by morphological erosion

3.3 Summary

The semantic segmentation network is used in encoder-decoder way to deal the vessel/OD segmentation from the background. The training images are artificially increased to provide the many example to fully train the network. The training and testing images are provided without prior pre-processing. The SegNet perform the pixel wise segmentation of the retinal images and provide the binary mask for the vessel. The class imbalance is compensated using median frequency balancing. In testing phase the SegNet output is bit dilated so, erosion is used to shrink and refine the segmentation.

Chapter 4

Experimental Results

4.1 Introduction

4.1.1 Database

To verify the proposed method reliability and performance publicly available retinal images are used for both vessels and OD. To analytically compare its results with the existing approaches we use two famous publicly available datasets DRIVE and MESSIDOR for vessels segmentation and optical disc segmentation respectively.

4.1.2 DRIVE Database

The photographs for the DRIVE database were obtained from a diabetic retinopathy screening program in The Netherlands. The screening population consisted of 400 diabetic subjects between 25-90 years of age.

All the images contained in the database were actually used for making clinical diagnoses. To ensure the utmost protection of patient privacy, information that might allow the identity of a patient to be reconstructed has been removed, and we have no actual knowledge that the images could be used alone or in combination to identify any subject.

Drive database consists of 40 labeled color images, where the manual annotation for the images are provided with the dataset. The training and testing images are already separated (20 training images, 20 testing images). The example image with corresponding ground truth are shown in Figure 4.1. In our experiments the 20-training image are used to create artificial images to support the better training. The data augmentation is used by image transformations like rotation, flipping, X-Y translation are used to create 1400 image-ground truth pairs. In other words, from each training image 70 artificial samples are generated. We have 30 images and increased the number of images by using augmentation. Also, in order to save computational resources, the images are resized to 447x447.

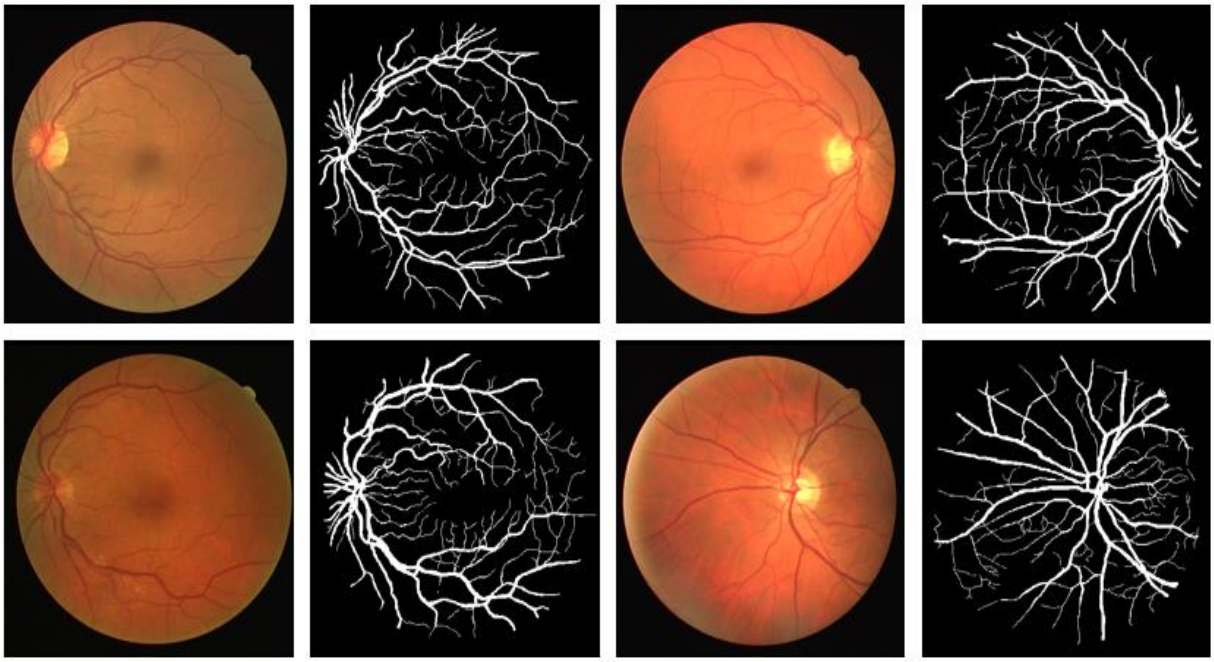

Figure 4.1: Example image for DRIVE dataset with corresponding ground truth

4.1.3 MESSIDOR Database

MESSIDOR database consists of 1200 color images with three different resolutions of 1140 × 1960, 2240 × 1488 and 2304 × 1536 pixels. Three ophthalmologic departments were involved for acquiring these images. In our experiment with MESSIDOR dataset, from the total image half images are used for training and rest half are used for training. In order to provide more images for the training the network artificial images are created by the data augmentation explained in section 4.1.2 for DRIVE dataset. By the said transformation 4800 image are created from the 600 training images. In other words, from each training image-ground truth pair eight artificial images are created in order to provide the variety features to the network during the process of training.

In order to save the computational resources all, the images are resized to 384 × 365.

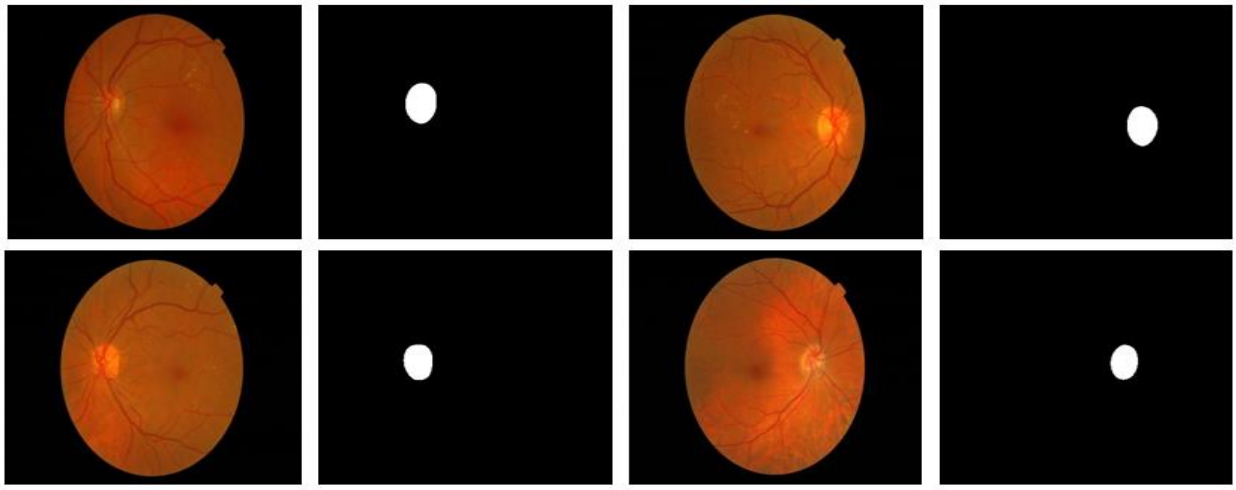

Figure 4.2: Example image for MESSIDOR dataset with corresponding ground truth

4.1.4 Experimental Environment

This study focus on semantic segmentation of vessel/OD in the retinal images, the method is based on deep learning approach so training and testing cannot be performed on ordinary system so GPU based system is required for the extensive training of the proposed network. In our experiments the training and testing performed on Intel Core i7 3.2 GHZ 8th generation CPU with 64 GB of system RAM and NVIDIA GeForce GTX 1080 [61]. It comes with 8 GB of graphics memory. The training and testing are performed with MATLAB 2018b [62].

4.1.5 Results for DRIVE dataset for vessel segmentation

In order to represent the segmentation performance visually the Figure 4.3 represent the results with DRIVE dataset. True positive pixel are the pixels which are vessel pixels in ground truth and correctly predicted by the network as vessel pixel (represented by blue color in the results in Figure 4.3). False negative are the pixels which are vessel pixels according to ground truth and falsely predicted as non-vessel by the network (represented by green color in the results in Figure 4.3).

The Table 1 represent the show association for the DRIVE dataset with existing approches considering the following evaluation matrics of sensitivity, specificity and accuracy.

$$Se = \frac{tp}{tp+fn} \tag{1}$$

$$Sp = \frac{tn}{tn+f\mathrm{p}} \tag{2}$$

$$Acc = \frac{tp+tn}{tp+fp+fn+tn} \tag{3}$$

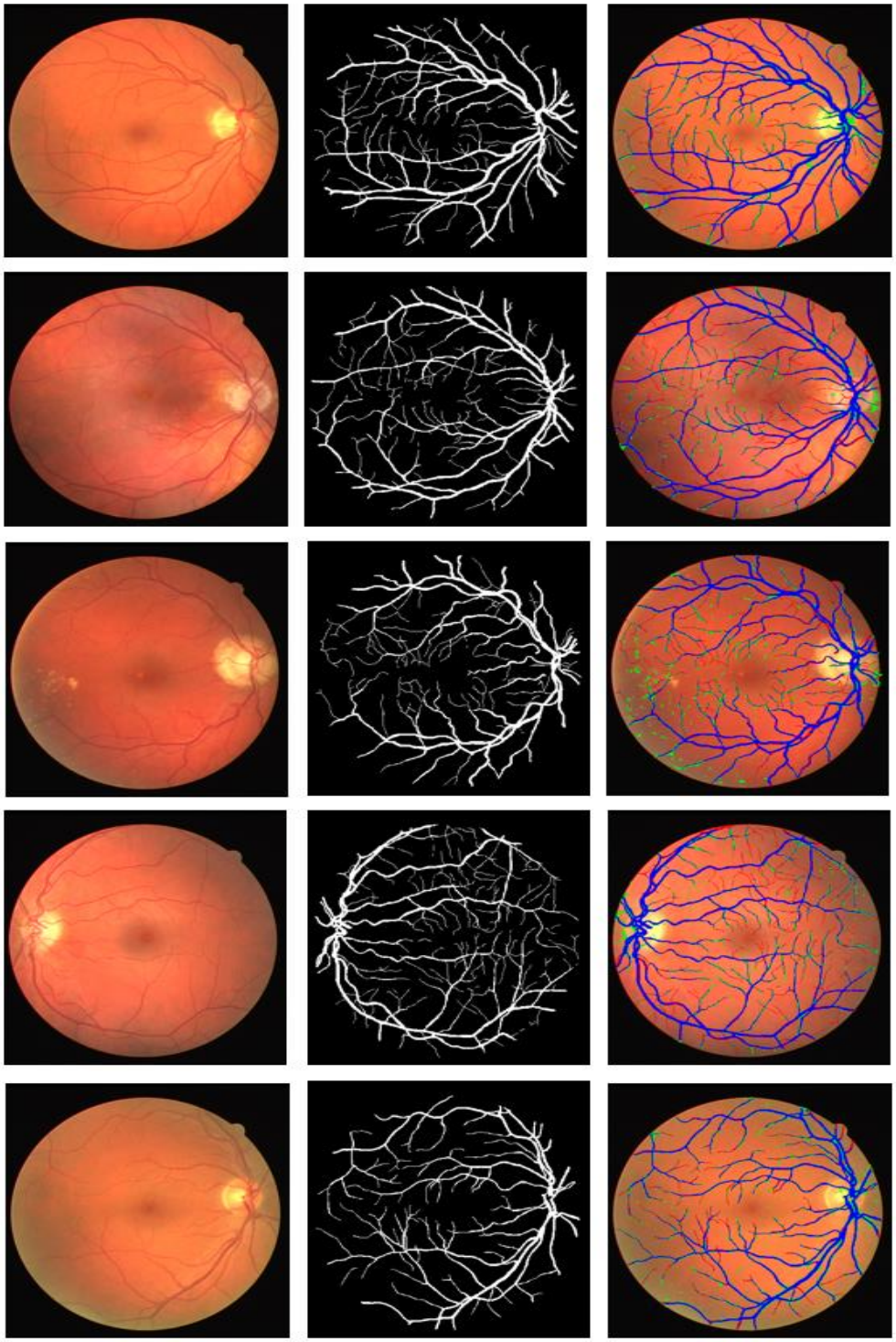

Figure 4.3: Samples of vessels segmentation by SegNet for DRIVE database (a) Original image (b) Ground Truth Mask (c) Segmented image by SegNet (True positive pixels are presented in blue, green and red presented false positive and negative respectively.

Table 3: Vessels segmentation performance measures

Performance Measures	Sensitivity	Specificity	Accuracy
Mendonca et al [49]	0.734	0.976	0.855
Matinez-Perez et al [50]	0.724	0.965	0.934
Palomera-Perez et al [51]	0.66	0.961	0.922
Soares et al. [52]	-	-	0.946
Zhao et al [53]	0.716	0.978	0.944
Orlando et al. [54]	0.785	0.967	-
Soomro et al. [39]	0.746	0.917	0.948
Soomro et al. [40]	0.739	0.956	0.948
Proposed Method	**0.76**	**0.97**	**0.95**

4.1.6 Results for MESSIDOR dataset for OD segmentation

In order to represent the segmentation performance visually the Figure 4.4 represent the results with MESSIDOR dataset. True positive pixel are the pixels which are vessel pixels in ground truth and correctly predicted by the network as vessel pixel (represented by blue color in the results in Figure 4.4). False negative are the pixels which are vessel pixels according to ground truth and falsely predicted as non-vessel by the network (represented by green color in the results in Figure 4.4).

The Table 2 represent the performance comparison for the DRIVE dataset with existing approches considering the following evaluation matrics of sensitivity, specificity and accuracy eleborated in section 4.1.2.

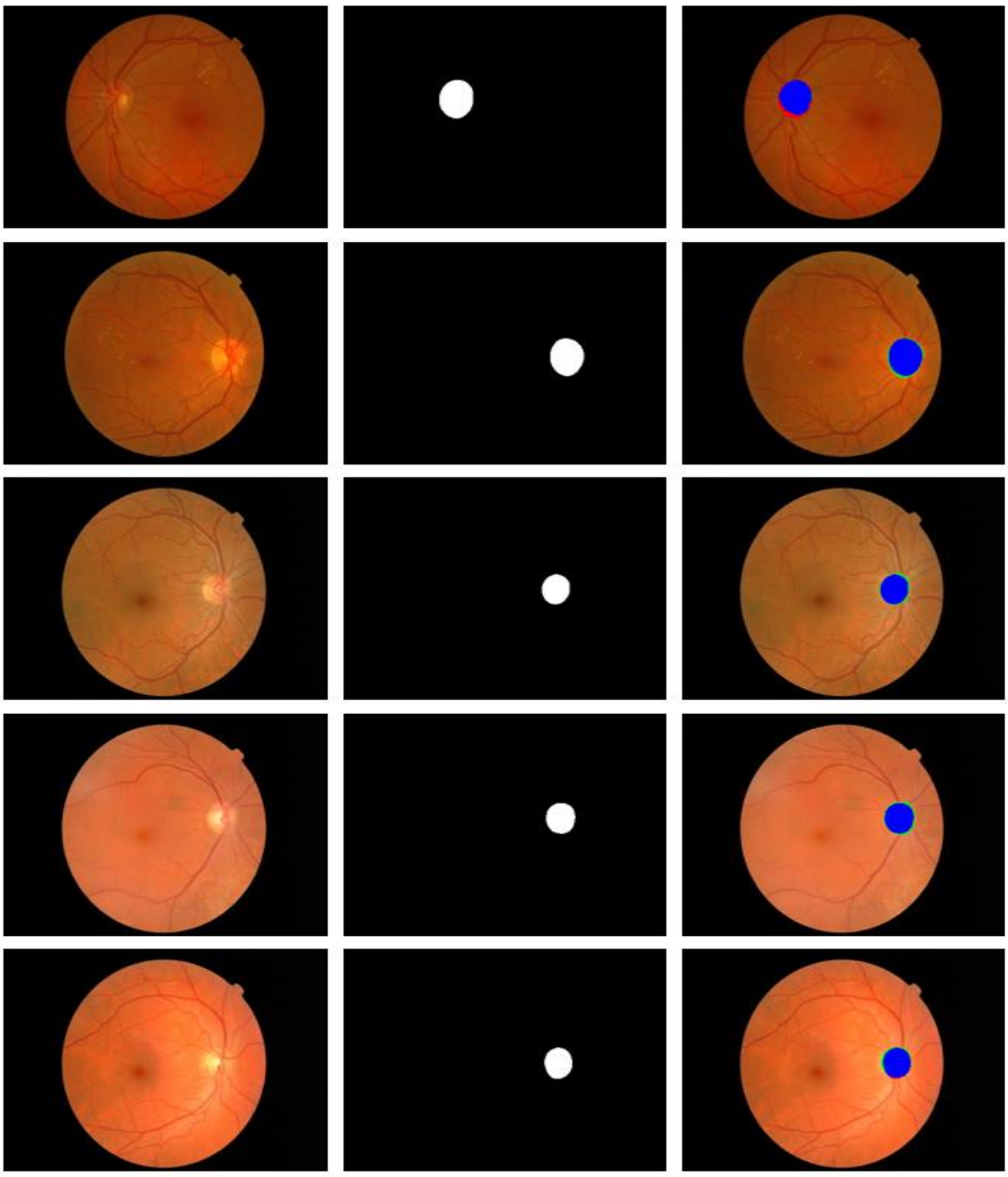

Figure 4.4: Samples of OD segmentation by SegNet for DRIVE database (a) Original image (b) Ground Truth Mask (c) Segmented image by SegNet (True positive pixels are presented in blue, green and red presented false positive and negative respectively.

Table 4: OD segmentation performance measures

Performance Measures	Sensitivity	Specificity	Accuracy
Morales et al. [55]	0.93	-	0.9949
Fan et al. [45]	0.9212	-	0.977
Abdullah et al. [56]	0.8954	0.9995	0.9989
Zahoor & Faraz. [44]	0.889	0.997	0.991
Rehman et al.[43]	0.948	0.988	0.988
Proposed Method	**0.9741**	**0.9988**	**0.9997**

Chapter 5

Conclusions and Perspectives

5.1 Conclusion

To check the effectiveness of the proposed scheme, we tested it on two datasets, DRIVE and MESSIDOR. From experimental results we found that the performance of proposed method is better than existing state of the art method.

As the proposed image enhancement is based on dividing image into different regions and optic disc, vessels. Therefore, the enhancement is totally dependent on the optic disc and vessles detection accuracy. This thesis propose a method which is recently different from others one and it is for the automatic segmentation and detection of the OD, Vessels in retinal images. The method presented a robust approach for optic disc and vessels localization. For localization of OD and Vessels, the image is first de-hazed and then using morphological operation a most eccentric region is found.

This method is proposed with the aim to design an algorithm that can facilitate us in designing the automated method for screening of Glaucoma. In the diagnoses of Glaucoma, the correct segmentation of OD is important and the major step which indicates the presence of Glaucoma. Although there are many approaches that have been employed earlier but the proposed algorithm achieves the higher accuracy as well as sensitivity which is vital for the correct diagnosis of the ailment. Although this algorithm performs well in comparison with the existing state of art and there are many challenges that have been addressed still there is no bound. There are many other factors and parameters as well that need to be considered in order to make the system efficient and economical. Therefore, in future we can improve the system by achieving its accuracy 100 percent.

In case of proposed deep learning method OD and vessels are segmented for the screening of Glaucoma. The segmentation of OD and vessels is performed using deep learning. The semantic segmentation is employed for the segmentation purpose. Initially the 1100 images of DRIVE dataset is used for the training and rest of the 100 images are used for the testing. Data augmentation is performed by using different operations including horizontal flipping, vertical flipping and rotation, in order to increase the number of images. The accuracy of the training increases with the increase in number of training images as classifier learns maximum the features in training. After the augmentation of the data input images are fed to the convolutional network which produces the feature vector. In this network VGG- 16 is used for the classification of three classes, i.e. Vessels, and Optic disc. The produced feature vectors go to the Soft Max classifier that classifies each pixel of these three classes and segmented the OD, vessels, and the background.

5.2 Perspective

OD, Vessels localization and segmentation is a preliminary phase in order to develop an automated method for radiography disease screening. The accuracy of OD and Vessels segmentation expands the right classification of radiography disease like hemorrhages, glaucoma etc. Similarly, OD and vessels localization is a preliminary step for accurate segmentation and localization that would leads towards promising segmentation results.

Optic disc and vessels segmentation is not only an essential step for our enhancement module but it is also a primary step to development of an automatic screening systems. The accuracy of the segmentation of optical disc and blood vessels method can improve the correct recognition of pathological diseases like glaucoma.

Our aim is to develop the automated method for glaucoma screening from this contribution that is under development. Even though related published works can be used, our work shows high accuracy, tolerated for different varieties of low contrast images and easy to integrate it for glaucoma and other radiography lesions systems. In future, our aim is to further enhance the method for real-time software application and make possible the functionality in modules for different types of retinography lesions localization programs. The proposed method successfully localizes the OD and Vessels that is a first step for glaucoma screening.

Bibliography

[1] M. Niemeijer *et al.*, "Retinopathy online challenge: automatic detection of microaneurysms in digital color fundus photographs," *IEEE Trans. Med. Imaging*, vol. 29, no. 1, pp. 185–195, 2010.

[2] P. D. Malaysia, "Clinical practice guidelines (CPG) management of type 2 diabetes mellitus," *Minist. Heal. Malaysia, Malaysian Endocr. Metab. Soc. Acad. Med. Malaysia*, vol. 1, p. 1000, 2009.

[3] X. Xu, W. Ding, M. D. Abràmoff, and R. Cao, "An improved arteriovenous classification method for the early diagnostics of various diseases in retinal image," *Comput. Methods Programs Biomed.*, vol. 141, pp. 3–9, 2017.

[4] T. A. Soomro, J. Gao, T. Khan, A. F. M. Hani, M. A. U. Khan, and M. Paul, "Computerised approaches for the detection of diabetic retinopathy using retinal fundus images: a survey," *Pattern Anal. Appl.*, vol. 20, no. 4, pp. 927–961, 2017.

[5] M. E. Brezinski *et al.*, "Imaging of coronary artery microstructure (in vitro) with optical coherence tomography," *Am. J. Cardiol.*, vol. 77, no. 1, pp. 92–93, 1996.

[6] G. A. Williams, I. U. Scott, J. A. Haller, A. M. Maguire, D. Marcus, and H. R. McDonald, "Single-field fundus photography for diabetic retinopathy screening: a report by the American Academy of Ophthalmology," *Ophthalmology*, vol. 111, no. 5, pp. 1055–1062, 2004.

[7] M. Siddiqui, "Optical domain subsampling for data-efficient optical coherence tomography (OCT)," Massachusetts Institute of Technology, 2013.

[8] S. N. Patel *et al.*, "Color fundus photography versus fluorescein angiography in identification of the macular center and zone in retinopathy of prematurity," *Am. J. Ophthalmol.*, vol. 159, no. 5, pp. 950–957, 2015.

[9] D. H. Hubel, *Eye, brain, and vision*. Scientific American Library/Scientific American Books, 1995.

[10] H. Kolb, "How the retina works: Much of the construction of an image takes place in the retina itself through the use of specialized neural circuits," *Am. Sci.*, vol. 91, no. 1, pp. 28–35, 2003.

[11] D. Huang *et al.*, "Optical coherence tomography," *Science (80-.).*, vol. 254, no. 5035, pp. 1178–1181, 1991.

[12] H. A. Quigley and A. T. Broman, "The number of people with glaucoma worldwide in 2010 and 2020," *Br. J. Ophthalmol.*, vol. 90, no. 3, pp. 262–267, 2006.

[13] Z. Zhang *et al.*, "Origa-light: An online retinal fundus image database for glaucoma analysis and research," in *2010 Annual International Conference of the IEEE Engineering in Medicine and Biology*, 2010, pp. 3065–3068.

[14] H. Noh, S. Hong, and B. Han, "Learning Deconvolution Network for Semantic Segmentation," in *2015 IEEE International Conference on Computer Vision (ICCV)*, 2015, pp. 1520–1528.

[15] V. Badrinarayanan, A. Kendall, and R. Cipolla, "Segnet: A deep convolutional encoder-decoder architecture for image segmentation," *IEEE Trans. Pattern Anal. Mach. Intell.*, vol. 39, no. 12, pp. 2481–2495, 2017.

[16] W. Yu, K. Yang, Y. Bai, T. Xiao, H. Yao, and Y. Rui, "Visualizing and comparing AlexNet and VGG using deconvolutional layers," in *Proceedings of the 33 rd International Conference on Machine Learning*, 2016.

[17] P. Ballester and R. M. Araujo, "On the performance of GoogLeNet and AlexNet applied to sketches," in *Thirtieth AAAI Conference on Artificial Intelligence*, 2016.

[18] S. Jégou, M. Drozdzal, D. Vazquez, A. Romero, and Y. Bengio, "The one hundred layers tiramisu: Fully convolutional densenets for semantic segmentation," in *Proceedings of the IEEE Conference on Computer Vision and Pattern Recognition Workshops*, 2017, pp. 11–19.

[19] M. Cordts *et al.*, "The cityscapes dataset for semantic urban scene understanding," in *Proceedings of the IEEE conference on computer vision and pattern recognition*, 2016, pp. 3213–3223.

[20] S. Akbar, M. U. Akram, M. Sharif, A. Tariq, and U. ullah Yasin, "Arteriovenous ratio and papilledema based hybrid decision support system for detection and grading of hypertensive retinopathy," *Comput. Methods Programs Biomed.*, vol. 154, pp. 123–141, 2018.

[21] A. Bhuiyan, M. A. Hussain, T. Y. Wong, and R. Klein, "Retinal Artery and Vein Classification for Automatic Vessel Caliber Grading," in *2018 40th Annual International Conference of the IEEE Engineering in Medicine and Biology Society (EMBC)*, 2018, pp. 870–873.

[22] R. Kurniawan, N. Yanti, M. Z. Nazri, and others, "Expert systems for self-diagnosing of eye diseases using Na{\"\i}ve Bayes," in *Advanced Informatics: Concept, Theory and Application (ICAICTA), 2014 International Conference of*, 2014, pp. 113–116.

[23] K. N. Fatima, M. U. Akram, and S. A. Bazaz, "Papilledema Detection in Fundus Images Using Hybrid Feature Set," in *2015 5th International Conference on IT Convergence and Security (ICITCS)*, 2015, pp. 1–4.

[24] K. Yousaf, M. U. Akram, U. Ali, and S. A. Sheikh, "Assessment of papilledema using fundus images," in *Imaging Systems and Techniques (IST), 2016 IEEE International Conference on*, 2016, pp. 476–481.

[25] R. Estrada, M. J. Allingham, P. S. Mettu, S. W. Cousins, C. Tomasi, and S. Farsiu, "Retinal artery-vein classification via topology estimation," *IEEE Trans. Med. Imaging*, vol. 34, no. 12, pp. 2518–2534, 2015.

[26] B. Dashtbozorg, A. M. Mendonça, and A. J. C. Campilho, "An automatic graph-based approach for artery/vein classification in retinal images.," *IEEE Trans. Image Process.*, vol. 23, no. 3, pp. 1073–1083, 2014.

[27] S. G. Vázquez *et al.*, "Improving retinal artery and vein classification by means of a minimal path approach," *Mach. Vis. Appl.*, vol. 24, no. 5, pp. 919–930, 2013.

[28] D. Relan, T. MacGillivray, L. Ballerini, and E. Trucco, "Retinal vessel classification: sorting arteries and veins," in *2013 35th Annual International Conference of the IEEE Engineering in Medicine and Biology Society (EMBC)*, 2013, pp. 7396–7399.

[29] M. Niemeijer *et al.*, "Automated measurement of the arteriolar-to-venular width ratio in digital color fundus photographs," *IEEE Trans. Med. Imaging*, vol. 30, no. 11, pp. 1941–1950, 2011.

[30] Q. Mirsharif, F. Tajeripour, and H. Pourreza, "Automated characterization of blood vessels as arteries and veins in retinal images," *Comput. Med. Imaging Graph.*, vol. 37, no. 7–8, pp. 607–617, 2013.

[31] C. Muramatsu, Y. Hatanaka, T. Iwase, T. Hara, and H. Fujita, "Automated detection and classification of major retinal vessels for determination of diameter ratio of arteries and veins," in *Medical Imaging 2010: Computer-Aided Diagnosis*, 2010, vol. 7624, p. 76240J.

[32] A. Pachiyappan, U. N. Das, T. V. S. P. Murthy, and R. Tatavarti, "Automated diagnosis of diabetic retinopathy and glaucoma using fundus and OCT images," *Lipids Health Dis.*, vol. 11, no. 1, p. 73, 2012.

[33] V. K. Jestin and R. R. Nair, "Extraction of Retinal Blood Vessels and Optic Disk for Eye Disease Classification," in *Proceedings of Fifth International Conference on Soft Computing for Problem Solving*, 2016, pp. 573–584.

[34] U. R. Acharya, N. Kannathal, E. Y. K. Ng, L. C. Min, and J. S. Suri, "Computer-based classification of eye diseases," in *Engineering in Medicine and Biology Society, 2006. EMBS'06. 28th Annual International Conference of the IEEE*, 2006, pp. 6121–6124.

[35] A. F. M. Oliveira, S. R. M. Pereira, and C. A. B. Silva, "Retinal Vessel Segmentation based on Fully Convolutional Neural Networks," *Expert Syst. Appl.*, 2018.

[36] M. Li, Q. Yin, and M. Lu, "Retinal Blood Vessel Segmentation Based on Multi-Scale Deep Learning," in *2018 Federated Conference on Computer Science and Information Systems (FedCSIS)*, 2018, pp. 1–7.

[37] M. A. U. Khan, T. A. Soomro, T. M. Khan, D. G. Bailey, J. Gao, and N. Mir, "Automatic retinal vessel extraction algorithm based on contrast-sensitive schemes," in *2016 International Conference on Image and Vision Computing New Zealand (IVCNZ)*, 2016, pp. 1–5.

[38] T. A. Soomro, M. A. U. Khan, J. Gao, T. M. Khan, M. Paul, and N. Mir, "Automatic Retinal Vessel Extraction Algorithm," in *2016 International Conference on Digital Image Computing: Techniques and Applications (DICTA)*, 2016, pp. 1–8.

[39] T. A. Soomro, M. A. U. Khan, J. Gao, T. M. Khan, and M. Paul, "Contrast normalization steps for increased sensitivity of a retinal image segmentation method," *Signal, Image Video Process.*, May 2017.

[40] T. A. Soomro, O. Hellwich, A. J. Afifi, M. Paul, J. Gao, and L. Zheng, "Strided U-Net

model: Retinal vessels segmentation using dice loss," in *2018 Digital Image Computing: Techniques and Applications (DICTA)*, 2018, pp. 1–8.

[41] C. Muramatsu *et al.*, "Automated segmentation of optic disc region on retinal fundus photographs: Comparison of contour modeling and pixel classification methods," *Comput. Methods Programs Biomed.*, vol. 101, no. 1, pp. 23–32, 2011.

[42] J. Cheng *et al.*, "Superpixel classification based optic disc and optic cup segmentation for glaucoma screening," *IEEE Trans. Med. Imaging*, vol. 32, no. 6, pp. 1019–1032, 2013.

[43] Z. U. Rehman, S. S. Naqvi, T. M. Khan, M. Arsalan, M. A. Khan, and M. A. Khalil, "Multi-parametric optic disc segmentation using superpixel based feature classification," *Expert Syst. Appl.*, vol. 120, pp. 461–473, 2019.

[44] M. N. Zahoor and M. M. Fraz, "Fast Optic Disc Segmentation in Retina Using Polar Transform," *IEEE Access*, vol. 5, pp. 12293–12300, 2017.

[45] Z. Fan *et al.*, "Optic Disk Detection in Fundus Image Based on Structured Learning," *IEEE J. Biomed. Heal. informatics*, vol. 22, no. 1, pp. 224–234, 2018.

[46] S. Morales, V. Naranjo, J. Angulo, and M. Alcañiz, "Automatic Detection of Optic Disc Based on PCA and Mathematical Morphology," *IEEE Trans. Med. Imaging*, vol. 32, no. 4, pp. 786–796, 2013.

[47] M. Abdullah, M. M. Fraz, and S. A. Barman, "Localization and segmentation of optic disc in retinal images using circular Hough transform and grow-cut algorithm, PeerJ, 4 (2016), e2003." 2003.

[48] J. Liu *et al.*, "Optic cup and disk extraction from retinal fundus images for determination of cup-to-disc ratio," in *2008 3rd IEEE Conference on Industrial Electronics and Applications*, 2008, pp. 1828–1832.

[49] D. W. K. Wong *et al.*, "Intelligent fusion of cup-to-disc ratio determination methods for glaucoma detection in ARGALI," in *2009 Annual International Conference of the IEEE Engineering in Medicine and Biology Society*, 2009, pp. 5777–5780.

[50] J. Cheng, F. Yin, D. W. K. Wong, D. Tao, and J. Liu, "Sparse dissimilarity-constrained coding for glaucoma screening," *IEEE Trans. Biomed. Eng.*, vol. 62, no. 5, pp. 1395–1403, 2015.

[51] R. GeethaRamani and C. Dhanapackiam, "Automatic localization and segmentation of Optic Disc in retinal fundus images through image processing techniques," in *2014 International Conference on Recent Trends in Information Technology*, 2014, pp. 1–5.

[52] A. Issac, M. P. Sarathi, and M. K. Dutta, "An adaptive threshold based image processing technique for improved glaucoma detection and classification," *Comput. Methods Programs Biomed.*, vol. 122, no. 2, pp. 229–244, 2015.

[53] M. D. Abramoff *et al.*, "Automated segmentation of the optic nerve head from stereo color photographs using biologically plausible feature detectors," *Investig. Ophthalmol. Vis. Sci.*, 2007.

[54] M. K. Dutta, A. K. Mourya, A. Singh, M. Parthasarathi, R. Burget, and K. Riha, "Glaucoma detection by segmenting the super pixels from fundus colour retinal images," in *2014 International Conference on Medical Imaging, m-Health and Emerging Communication Systems (MedCom)*, 2014, pp. 86–90.

[55] D. Sarkar and S. Das, "Automated Glaucoma detection of medical image using biogeography based optimization," in *Advances in Optical Science and Engineering*, Springer, 2017, pp. 381–388.

[56] T. Khalil, M. U. Akram, S. Khalid, and A. Jameel, "Improved automated detection of glaucoma from fundus image using hybrid structural and textural features," *IET Image Process.*, vol. 11, no. 9, pp. 693–700, 2017.

[57] G. Lim, Y. Cheng, W. Hsu, and M. L. Lee, "Integrated optic disc and cup segmentation with deep learning," in *2015 IEEE 27th International Conference on Tools with Artificial Intelligence (ICTAI)*, 2015, pp. 162–169.

[58] P. Liskowski and K. Krawiec, "Segmenting Retinal Blood Vessels With Deep Neural Networks," *IEEE Trans. Med. Imaging*, vol. 35, no. 11, pp. 2369–2380, 2016.

[59] A. M. Mendonca and Aa. Campilho, "Segmentation of Retinal Blood Vessels by Combining the Detection of Centerlines and Morphological Reconstruction," *IEEE Trans. Med. Imaging*, vol. 25, pp. 1200–1213, 2006.

[60] Martinez-Perez, H. AD, and T. SA, "Segmentation of blood vessels from red-free and fluorescein retinal images," *J. Med. Image Anal.*, vol. 11, no. 1, pp. 47–61, 2007.

[61] M. A. Palomera-Perez, M. E. Martinez-Perez, H. Benitez-Perez, and J. L. Ortega-Arjona, "Parallel Multiscale Feature Extraction and Region Growing: Application in Retinal Blood Vessel Detection," *IEEE Trans. Inf. Technol. Biomed.*, vol. 14, no. 2, pp. 500–506, 2010.

[62] J. V. B. Soares, J. J. G. Leandro, R. M. Cesar, H. F. Jelinek, and M. J. Cree, "Retinal vessel segmentation using the 2-D Gabor wavelet and supervised classification," *IEEE Trans. Med. Imaging*, vol. 25, no. 9, pp. 1214–1222, 2006.

[63] Y. Zhao, L. Rada, K. Chen, S. P. Harding, and Y. Zheng, "Automated Vessel Segmentation Using Infinite Perimeter Active Contour Model with Hybrid Region Information with Application to Retinal Images," *IEEE Trans. Med. Imaging*, vol. 34, no. 9, pp. 1797-1807., 2015.

[64] J. I. Orlando and M. Blaschko, "Learning fully-connected CRFs for blood vessel segmentation in retinal images," *Med. Image Comput. Comput. Assist. Interv. (MICCAI)*, vol. 17, pp. 634–641, 2014.

[65] S. Morales, V. Naranjo, J. Angulo, and M. Alcañiz, "Automatic detection of optic disc based on PCA and mathematical morphology," *IEEE Trans. Med. Imaging*, vol. 32, no. 4, pp. 786–796, 2013.

[66] M. Abdullah, M. M. Fraz, and S. A. Barman, "Localization and segmentation of optic disc in retinal images using circular Hough transform and grow-cut algorithm," *PeerJ*, vol. 4, p. e2003, Apr. 2016.

[67] NVIDIA GeForce GTX 1080 https://www.nvidia.com/en-in/geforce/products/10series/geforce-gtx-1080-ti/ accessed on 10th July, 2019.

[68] MATLAB 2018b https://www.mathworks.com/downloads/ accessed on 10th July, 2019.